

## Supplementary Information: Exploring the Degradation of Silver Nanowire Networks under Thermal Stress by Coupling *In Situ* X-Ray Diffraction and Electrical Resistance Measurements

Laetitia Bardet,<sup>1,2</sup> Hervé Roussel,<sup>1</sup> Stefano Saroglia,<sup>1</sup> Masoud Akbari,<sup>1</sup> David  
Muñoz-Rojas,<sup>1</sup> Carmen Jiménez,<sup>1</sup> Aurore Denneulin,<sup>2</sup> and Daniel Bellet<sup>1,\*</sup>

<sup>1</sup>*Univ. Grenoble Alpes, CNRS, Grenoble INP, LMGP, F-38000, Grenoble, France*

<sup>2</sup>*Univ. Grenoble Alpes, CNRS, Grenoble INP, LGP2, F-38000, Grenoble, France*

---

\* daniel.bellet@grenoble-inp.fr

## I. SETUP TO MEASURE BOTH STRUCTURAL AND ELECTRICAL RESISTANCE PROPERTIES

Figure S1 shows the setup used to both *in situ* measure structural properties and electrical properties thanks to X-ray diffraction (XRD) and 2-probe electrical resistance measurements, respectively, during the thermal ramp. Figure S1a exhibits a schematic illustration of XRD setup. Figure S1b exhibits a hemispherical graphite dome used to close the chamber and cooled by compressed air for temperatures above 200 °C. Figure S1c exhibits a sample which is placed inside the chamber. Silver paste contacts (L-200N, CDS Electronique, France) were manually deposited on two opposite sides of the samples and dried at room temperature overnight.

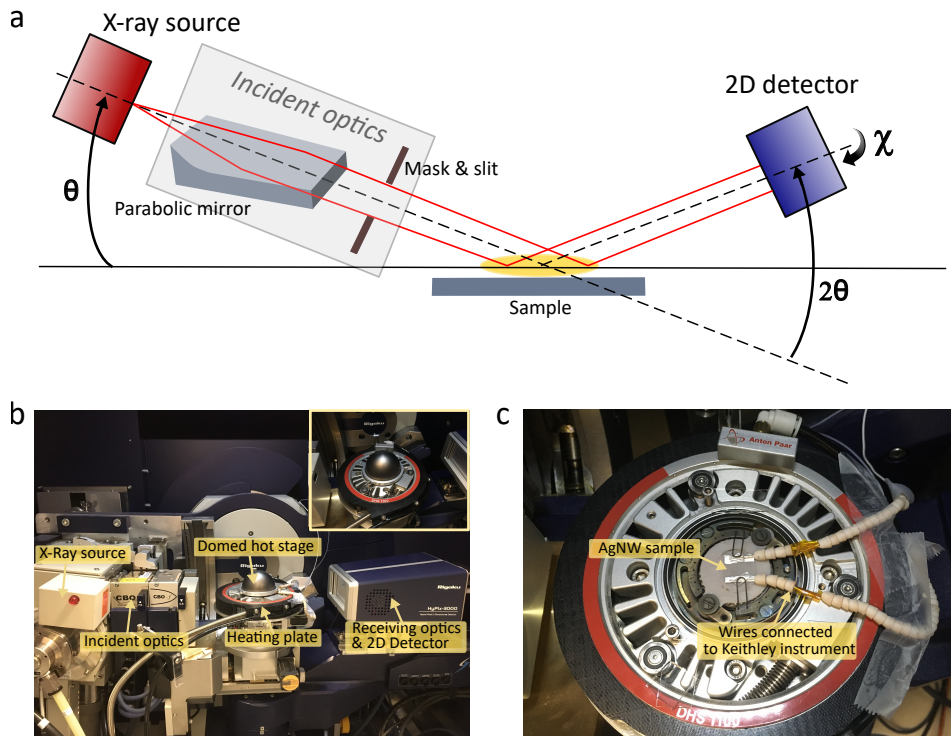


FIG. S1. Setup used to measure *in situ* structural and electrical properties. (a) Schematic illustration of the setup used to measure *in situ* X-Ray Diffraction (XRD) on AgNW networks. (b) Photo of the setup. The inset shows the dome covering the analyzed sample. (c) Zoom of the setup, without the dome, where can be observed the AgNW network with two cables connected to its edge for electrical resistance measurement by a 2-point probe.

## II. 1D INTEGRATION *VERSUS* 2D INTEGRATION

When working with textured films, the intensity values of XRD spectra strongly depend on the X-ray optical configuration, and thus the integration parameters of Debye rings. This is clearly illustrated in Figure S2a and b, in which 1D integration and 2D integration, respectively, of Debye rings of the same AgNW network are compared. For instance, the (200) Bragg peak exhibits a larger integrated intensity compared to the (111) peak for the 1D integration ( $|\chi| \leq 4^\circ$ ), while the inverse observation can be stated for the 2D integration ( $|\chi| \leq 24^\circ$ ). 1D integration data along the  $2\theta$  direction corresponds to a narrow acceptance domain in  $\chi$  value ( $|\chi| \leq 4^\circ$ ). Conversely, 2D integration corresponds to a larger acceptance domain in  $\chi$  value ( $|\chi| \leq 24^\circ$ ).

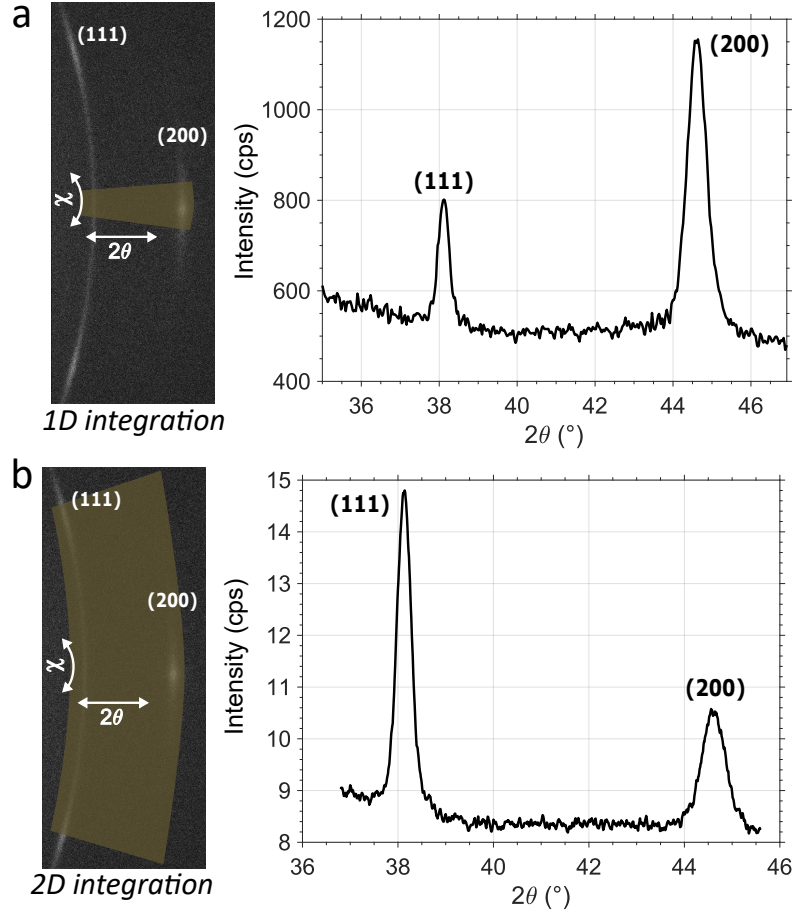


FIG. S2. Comparison between two XRD spectra associated with two different integrations of Debye rings. Debye rings and XRD spectra with (a) 1D integration and (b) 2D integration. The intensity was integrated along the  $2\theta$  direction (left) with two different  $\chi$  ranges:  $|\chi| \leq 4^\circ$  and  $|\chi| \leq 24^\circ$ , (1D and 2D integration, respectively) to obtain the resulting XRD spectrum (right).

### III. INFLUENCE OF THE DOME USED FOR THE HEATING STAGE ON XRD MEASUREMENTS

The thermal stage requires a graphite dome surrounding the sample to reduce thermal losses. However, Figure S3 shows that the Bragg peaks from the graphite and from AgNWs do not overlap.

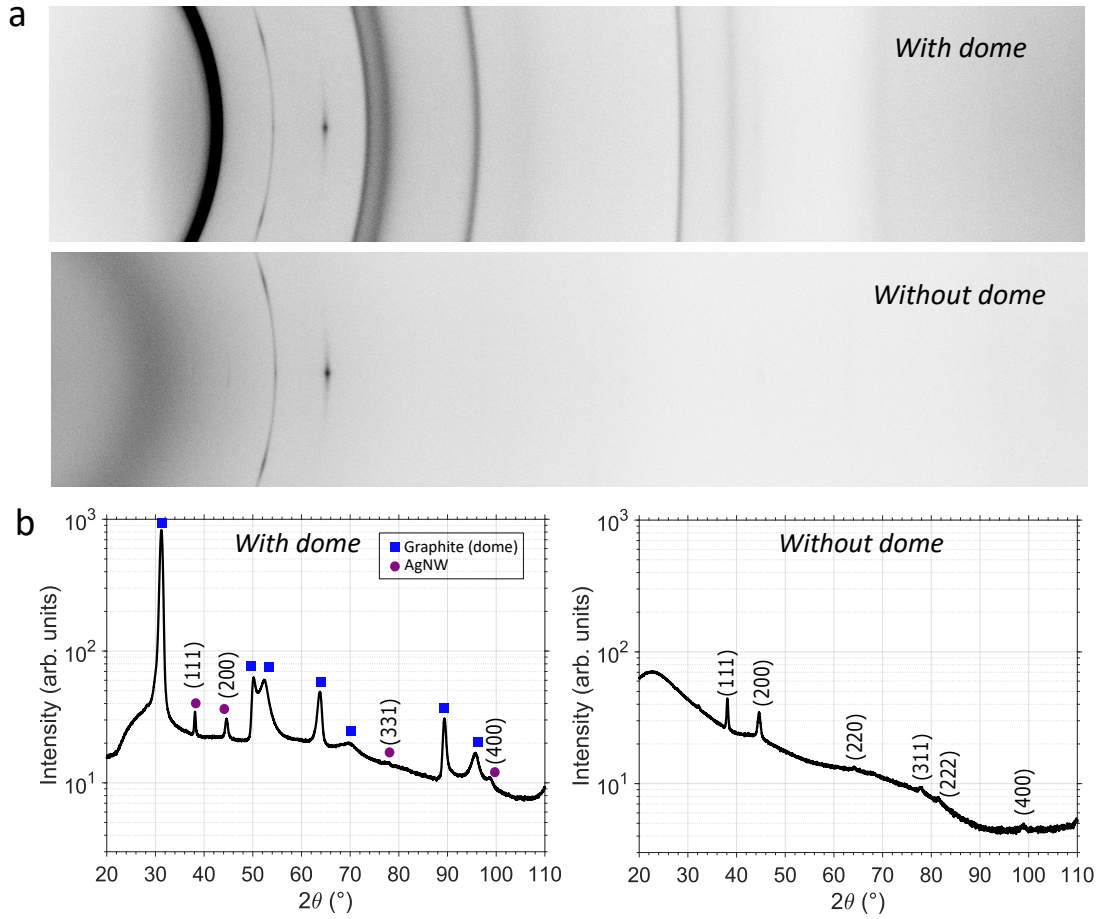


FIG. S3. **Influence of graphite dome on XRD measurements.** (a) Debye rings diagram of AgNW networks with a dome (top) and without dome (bottom) (b) XRD spectra of the Debye rings diagram (2D integration) with a dome (left) and without dome (right).

#### IV. DEBYE RINGS AND XRD SPECTRA BEFORE AND AFTER THERMAL RAMP

Figure S4d-f exhibit XRD spectra measured at 30 °C, plotted from Debye rings (Figure S4a-c), before and after a thermal ramp for the bare AgNW network, 15 nm-SnO<sub>2</sub>/AgNW network and 40 nm-SnO<sub>2</sub>/AgNW network, respectively. A significant change can be observed for the bare AgNW network (Figure S4a and d) compared to the 15 nm-SnO<sub>2</sub>/AgNW network and 40 nm-SnO<sub>2</sub>/AgNW network.

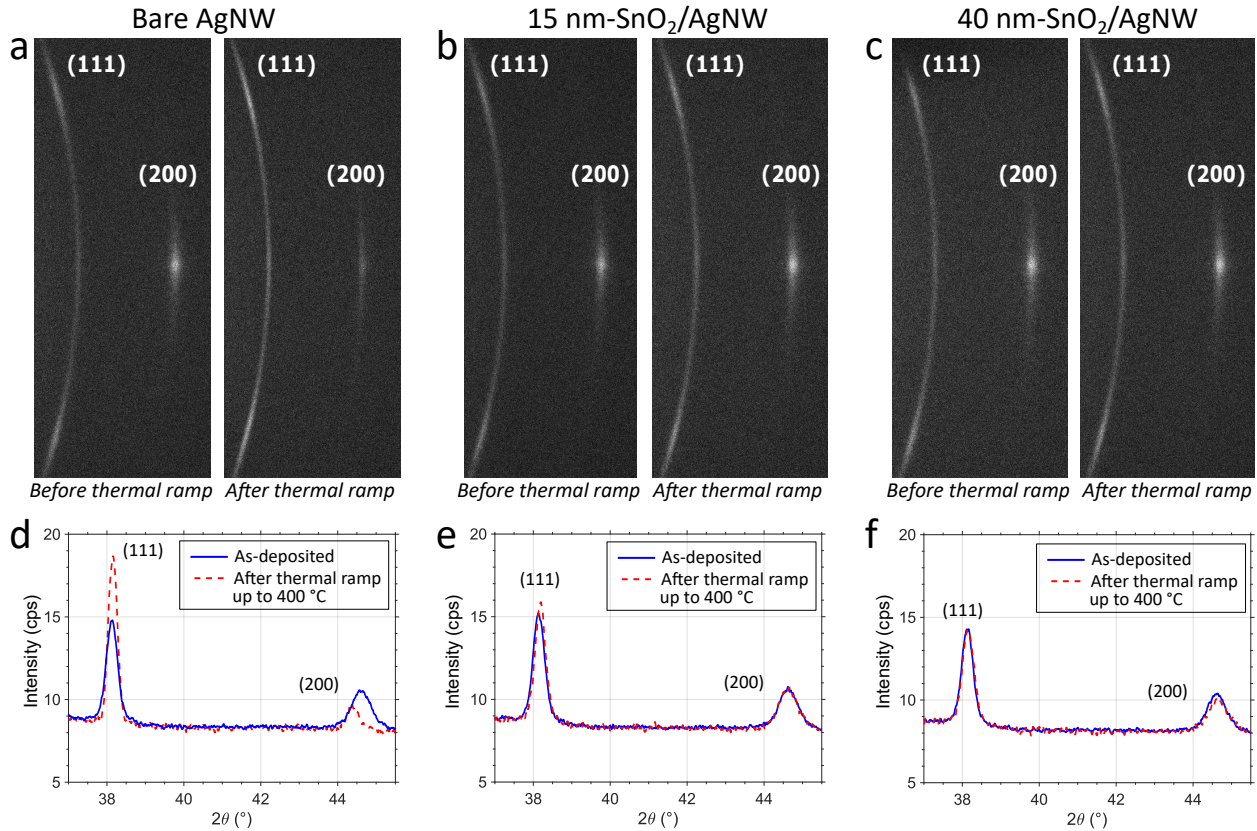


FIG. S4. Debye rings and XRD spectra of bare and SnO<sub>2</sub>-coated AgNW networks, before and after thermal stress. Debye rings of (111) and (200) planes for (a) the bare AgNW network, (b) 15 nm-SnO<sub>2</sub>/AgNW network and (c) 40 nm-SnO<sub>2</sub>/AgNW network before (left image) and after (right image) a thermal ramp, performed in air, up to 400 °C. XRD spectra measured at room temperature, for (d) the bare AgNW network, (e) 15 nm-SnO<sub>2</sub>/AgNW network and (f) 40 nm-SnO<sub>2</sub>/AgNW network, before (blue solid line) and after (red dashed line) a thermal ramp, performed in air, up to 400 °C. These XRD data are extracted from a-c, respectively.

## V. FINITE CRYSTAL DOMAIN

Thanks to the scheme depicted in Figure S5a, we estimate  $D_{111} \approx \frac{D_{NW}}{2\cos\alpha} \approx \frac{\sqrt{6}}{2}D_{NW} \approx 98$  nm with  $D_{NW} = 80$  nm and  $\theta_{111} = 19.03^\circ$ . According to the scheme depicted as in Figure S5b, we obtain  $D_{200} \approx \frac{D_{NW}}{2} = 40$  nm with  $\theta_{200} = 22.12^\circ$ .

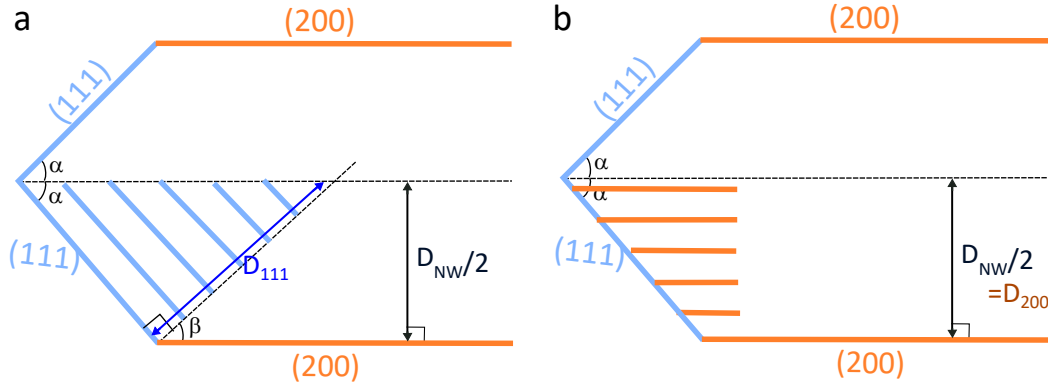


FIG. S5. Schematic illustration of the finite crystal domain size  $D_{hkl}$  for an ideal AgNW. The cross-section of a perfect AgNW along the [011] axis is illustrated for (a) (111) planes and for (b) (200) planes.